ZIBELINE INTERNATIONAL™ PUBLISHING

ISSN: 2616-4302 (Online)
CODEN: AMMCFL

Acta Mechanica Malaysia (AMM)

DOI: http://doi.org/10.26480/amm.01.2021.22.26

RESEARCH ARTICLE

NUMERICAL MODELING THE EFFECTS OF ADDITIVE MANUFACTURING PARAMETERS, HEAT TREATMENT AND ORIENTATION ON RESIDUAL STRESS AND DISTORTION OF METAL POWDER IN718 PUMP IMPELLER FABRICATION

Alireza M. Haghighi

Shahid Bahonar University of Kerman, Iran
Corresponding Author Email: m.haghighi.alireza@gmail.com

ARTICLE DETAILS

Article History:

Received 25 May 2021
Accepted 30 June 2021
Available online 9 July 2021

ABSTRACT

Selective laser melting (SLM) technology based on IN718 powder bed by means of finite element method (FEM) has been concerned with effects of additive manufacturing (AM) parameters, heat treatment and part orientation on residual stress and distortion of IN718 pump impeller. It is found that fabrication in horizontal position has the least and vertical position has the most residual stress and distortion between considered conditions. Also, increasing the speed of the process is very efficient and reduce the residual stress and distortion of the process up to 65% and heat treatment is beneficial in reducing the distortion in most of the conditions.

KEYWORDS

Selective Laser Melting, IN718, Pump Impeller, Finite Element Method.

1. INTRODUCTION

Laser powder bed fusion is a metal additive manufacturing process which is a very promising and popular technology for manufacturing large and complex lightweight components with good mechanical strength and low porosity for various industrial and construction applications (Levkulich et al., 2019; Li et al., 2018; Cao et al., 2016). Large thermal gradients and fast cooling rate during the solidification of each layer cause stresses appearance (Levkulich et al., 2019). The thermal stresses in elastic range release when the temperature recover, but the stresses exceed the yield limit, after solidification of the material remain in the component as residual stress which leads to distortion of the component (Li et al., 2018). The residual stress and distortion of repeated heating and cooling cycles have not been understood well yet, but predicting the greatness and distribution of these phenomena have direct effects on the efficiency and cost of manufacturing (Cao et al., 2016). FEM has a significant role in predicting these phenomena in order to minimize the experimentation needed to increase the quality and efficiency rate of the process (Cao et al., 2016).

IN718 is a nickel-chromium strengthened superalloy with high strength at elevated temperatures up to 650°C, good weldability, high fatigue and lower residual stress that make it popular in wide range of applications such as turbine disks, jet engines and pump impellers material (Wang et al., 2012; Zhang et al., 2010; Anderson et al., 2006). These properties make it difficult to manufacturing with conventional machining methods at room temperature because of excessive tool wear, poor surface finish and complex structure of IN718 components (Anderson et al., 2006; Attia et al., 2010; Costes et al., 2007).

Metal powder additive manufacturing is an appropriate method that reduce the cost and time of designing and fabrication without any specific tooling which make it a suitable choice for IN718 parts. Some parameters of the AM process such as beam width, speed and power of the machine, heat treatment and part orientation have significant roles in mitigating the residual stress and distortion. In order to study the effects of AM parameters on greatness and distribution of residual stress and distortion, researchers study different aspects of these phenomena. Several methods such as x-ray diffraction and contour method to investigate the effects of process parameters on residual stress and distortion in the laser power bed fusion of Ti-6Al-4V (Levkulich et al., 2019). It obtained that process parameters have a great influence on magnitude and distribution of these phenomena. A study developed a three-dimensional thermo-mechanical model of multi-track multi-layer SLM by means of FEM to model temperature and residual stress fields in SLM (Li et al., 2018). According to the results, residual stress increase in the direction of layer height with increasing the number of printed layers. However the maximum of von Mises stress is in the middle plane of printed part. A 3D thermo-mechanical model to investigate the residual stress and distortion in electron beam AM of Ti-6Al-4V build plates and validate it by experimental method. The results show that preheating at least twice has a significant effect on reduction of residual stress and distortion of the process (Cao et al., 2016). 3D thermo-mechanical model in laser sintering process of titanium alloy products to study temperature history, and residual stress behavior of single-layer and multi-layer of the process (Zhao et al., 2017). An evaluate residual stress of Ti-6Al-4V and Inconel 718 in SLM by means of contour and numerical method (Ahmad et al. 2018). Results show the concentration of tensile residual stress near the surface and compressive stresses at the center region of both material components. A physics-based model to investigate residual stress of AM of metallic materials and validated experimentally by X-ray measurements (Fergani et al., 2016). A research theoretical and experimental on residual stress of SLM and selective lase sintering processes. They found that upper layers consist large zone of tensile stress that at the surface of the part is equal to yield

Quick Response Code	Access this article online	
	Website: www.actamechanicamalaysia.com	**DOI:** 10.26480/amm.01.2021.22.26

Cite the Article: Alireza M. Haghighi (2021). Numerical Modeling the Effects of Additive Manufacturing Parameters, Heat Treatment and Orientation on Residual Stress and Distortion of Metal Powder In718 Pump Impeller Fabrication. *Acta Mechanica Malaysia, 4(1): 22-26*.

stress of the material and it decrease by reducing the Z value (Mercelis and Kruth, 2006). Also, they result that residual stress increase by adding more layer to the part, and it has a reverse relation with thickness of the base plate. An investigate the thermal distribution, the residual stress and deformation of metal AM by using a 3D sequentially coupled thermo-mechanical FEM by means of ABAQUS software and compare the results with experimental method (Liu et al., 2015). A 3D transient heat transfer and fluid flow model to simulate process of laser additive manufacturing accurately and predict residual stress and deformation with the least error than experimental method. Results show that reducing the layers thickness reduce the residual stresses significantly (Mukherjee et al., 2017). A recent study using adaptive mesh in 3D thermo-mechanical FEM of AM process present a new method that results show more accuracy in less time than conventional FEM (Hajializadeh and Ince, 2019).

2. Numerical Simulation Approach

2.1 Governing Equations

Thermo-mechanical coupled system has been used for finite element analyzing the process. The SLM and multi-layer laser welding are similar and obey the same rules. So, the moving Gaussian heat source of the laser welding can be applied on laser beam of the metal bed fusion process as (Bian et al., 2020; Wu et al., 2014):

$$q_{(r)} = \frac{2AP}{\pi\omega^2}\exp\left(-\frac{2r^2}{\omega^2}\right) \quad (1)$$

That q is the heat flux density, A is the laser absorptivity of the materials, P is the laser power, r is radial distance from the beam center, and ω is the radius of the beam. The transient temperature distribution equation is (Bian et al., 2020; Wu et al., 2014; Rashid et al., 2018):

$$\rho c_p \frac{\partial T}{\partial t} = \sum_{i=1}^{n} \nabla_i(-K\Delta T_i) \quad (2)$$

$$\frac{\partial(\rho c_p T)}{\partial t} = \frac{\partial}{\partial x}\left(k\frac{\partial T}{\partial x}\right) + \frac{\partial}{\partial y}\left(k\frac{\partial T}{\partial y}\right) + \frac{\partial}{\partial z}\left(k\frac{\partial T}{\partial z}\right) + Q \quad (3)$$

Where ρ, c, and K are the density, specific heat capacity and thermal conductivity respectively. i is the number of layers printed by SLM process and Q is the volumetric heat source per unit of the part (Aminifar and Haghighi, 2020).

The finite element software use hooks' law to obtain the stresses and strain. Strain is summation of elastic ε_e, plastic ε_p, and thermal strain ε_T as:

$$\sigma_{ii} = -E\frac{(1-\mu)\varepsilon_{jj} + \mu(\varepsilon_{ii} + \varepsilon_{kk}) - a_e T(1+\mu)}{(1+\mu)(-1+2\mu)} \quad (4)$$

$$\varepsilon = \varepsilon_e + \varepsilon_p + \varepsilon_T \quad (5)$$

Where μ and a_e are Poisson's ratio and coefficient of thermal expansion, respectively.

2.2 Finite Element Method

The pump impeller designed in AutoCAD software. The diameter is 432 mm and height of 89 mm with six blades. There are six screw holes and a key place on it in order to be fixed to the seal and shaft as showed in fig. 1:

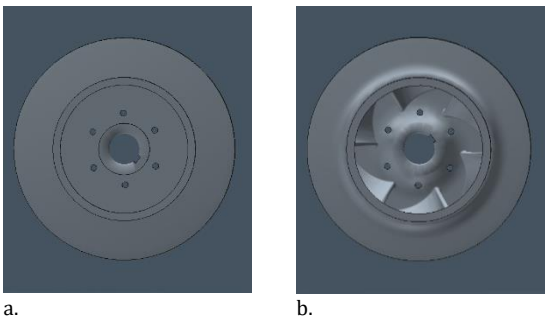

a. b.

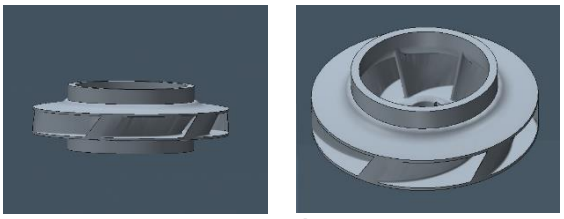

c. d.

Figure 1: Different view side of IN718 pump impeller model: a. Back view, b. Front view, c. Side view, d. Isometric view

The STL file of the designed part imported to the Simufact Additive software. Three orientation of 0, 45 and 70 degree have been considered in this investigation. In each orientation, sufficient supports have been considered. Volumetric mesh for main part and supports with voxel size of 3.2 mm and minimum fraction of 5% have been considered for each orientation. Fig. 2 shows supports for model in 45 degree, and table 1 shows number of considered supports and volumetric mesh elements for each orientation.

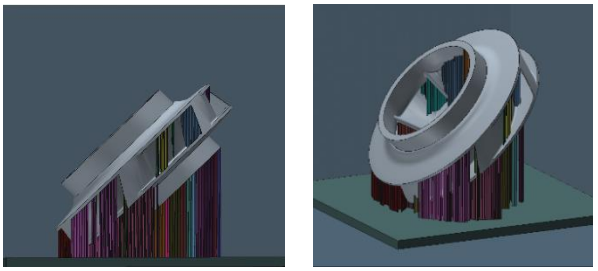

a. b.

Figure 2: Supports for AM of IN718 pump impeller in 45 degree

Table 1: Number of considered supports and volumetric mesh elements for each orientation.

	0°	45°	70°	90°
Num. of Supports	10	96	24	23
Num. of Volumetric Mesh Elements	72522	69833	64250	63319

2.3 Assumptions

The AM process of manufacturing IN718 pump impeller simulated by characteristics of SLM 280HL machine specifically with initial speed of 1 m/s and power of 200 W. In all investigated conditions, efficiency rate and beam width have been assumed 0.6 and 0.15 mm, respectively, with layer thickness of 0.03 mm. Heat treatment has been applied to the part and supports. Fig. 3 shows the heating chart inserted to the fabricated part to investigate the effects of heat treatment on the main part.

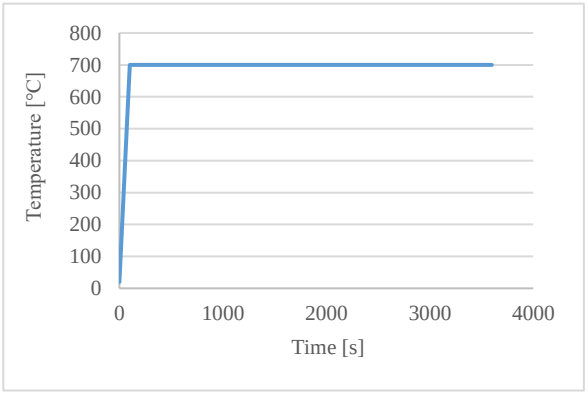

Figure 3: Data diagram of heat treatment inserted to the part and supports

Also, it assumed that the manufactured part and supports have been cut off from the base plate immediately without any condition simulation. Furthermore, total supports have been removed from the manufactured part instantly in one stage.

3. Results and Discussion

In the following sections, analysis of AM parameters, part orientation and heat treatment on residual stress and distortion of IN718 pump impeller by means of FEM has be discussed. Also, manufacturing parameters including power and speed of the machine have been changed ±20% from the initial values in order to study effects of AM parameters on distribution of residual stress and distortion.

Table 2 shows considered situations and conditions of SLM process and table 3 shows the effect of heat treatment on considered conditions. Max. of residual stress and distortion of each condition and Max. of displacement of layers in printing direction have been specified.

3.1 Effects of Part Orientation

According to table 2, and 3 manufacturing the IN718 pump impeller in 0 degree has the least and 90 degree fabrication has the most residual stress between considered conditions. Fig. 4.a shows the Max. of residual stress in different conditions. Distortion results is a little complicated than residual stress. In condition 1, distortion distribution is approximately equal in all considered conditions, but in condition 2, manufacturing in 0 degree has the least and 70 degree has the most distortion. Fig. 4.b shows the Max. distortion in all considered conditions. Fig. 4.c shows AM-layer displacement in 0 degree is much lower than other conditions and in 70 degree has the highest displacement. According to the results of all conditions, manufacturing the pump in 0 degree have the least residual stress, distortion and layers displacement.

Table 2: Results of manufacturing in different orientations and AM parameters without heat treatment

Orientation	Condition	Power $[W]$	Speed $[m/s]$	Max. of Residual Stress $[MPa]$	Max. of Distortion $[mm]$	Max. of AM-layer Displacement $[mm]$
0	1	200	1	1009.34	2.40	0.08
	3	240	1	892.79	1.89	0.04
	5	200	1.20	828.93	1.59	0.02
	7	160	1	823.25	1.56	0.02
	9	200	0.80	900.78	1.96	0.04
45	1	200	1	1047.76	2.56	0.23
	3	240	1	986.50	1.41	0.10
	5	200	1.20	921.72	0.96	0.07
	7	160	1	914.07	0.92	0.06
	9	200	0.80	992.95	1.49	0.11
70	1	200	1	1059.49	3.22	0.36
	3	240	1	1028.97	1.65	0.16
	5	200	1.20	985.82	1.11	0.11
	7	160	1	979.74	1.06	0.10
	9	200	0.80	1032.41	1.73	0.17
90	1	200	1	1059.42	2.59	0.38
	3	240	1	1046.66	1.36	0.14
	5	200	1.20	1013.05	0.89	0.09
	7	160	1	1007.38	0.85	0.09
	9	200	0.80	1048.88	1.43	0.15

Table 3: Results of manufacturing in different orientations and AM parameters with heat treatment.

Orientation	Condition	Power $[W]$	Speed $[m/s]$	Max. of Residual Stress $[MPa]$	Max. of Distortion $[mm]$	Max. of AM-layer Displacement $[mm]$
0	2	200	1	1013.98	1.34	0.09
	4	240	1	994.54	1.62	0.04
	6	200	1.20	993.55	1.38	0.02
	8	160	1	993.59	1.39	0.02
	10	200	0.80	998	1.37	0.04
45	2	200	1	1046.86	2.89	0.25
	4	240	1	1020.35	2.29	0.11
	6	200	1.20	1016.89	2.13	0.07
	8	160	1	1016.55	2.13	0.07
	10	200	0.80	1020.87	2.32	0.11
70	2	200	1	1059.58	4.18	0.40
	4	240	1	1029.16	2.57	0.17
	6	200	1.20	996.28	2.35	0.11
	8	160	1	996.30	2.35	0.11
	10	200	0.80	1032.66	2.64	0.18
90	2	200	1	1060	3.47	0.34
	4	240	1	1045.08	2.38	0.15
	6	200	1.20	1034.03	2.33	0.10
	8	160	1	1033.83	2.33	0.09
	10	200	0.80	1047.34	2.40	0.16

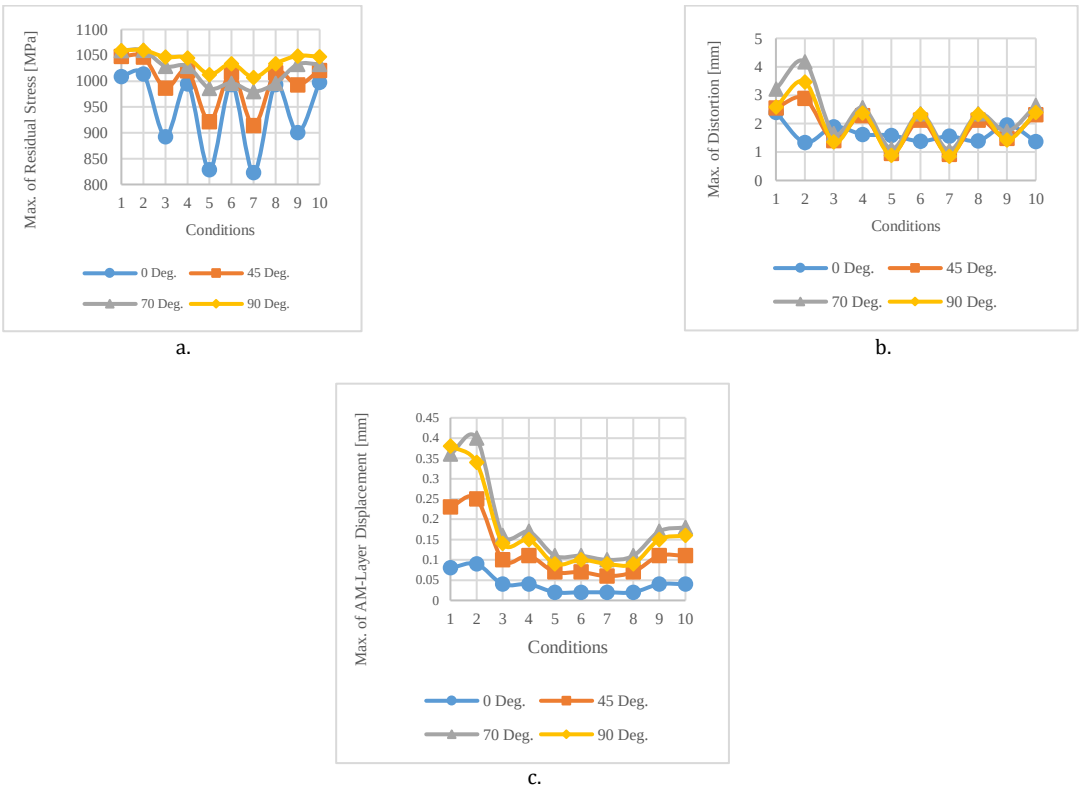

Figure 4: a. Max. of Residual Stress, b. Max. of Distortion, c. Max. of AM-Layer Displacement

3.2 Effects of AM Parameters

By 20% increasing the speed, residual stresses reduce 33.75% in 0 degree from the initial condition and difference continuously ascending to 65.63% at 90 degree. In this condition, distortion reduces for about 34% in 0 degree to 65% in 90 degree from the initial condition. By 20% reducing the speed, the Max. of residual stresses decrease 10.75% in 0 degree and by getting close to 90 degree, residual stress increase and difference declines to 1%. Distortion reduces from 18.33% in 0 degree to about 45% in 70 and 90 degree from the initial condition.

Power changes have similar effects on residual stresses and distortion. By 20% adding to the power, Max. of residual stresses decline 11.54% in 0 degree, but by increasing the angle of the main part, the residual stresses increase and the difference become 1% in 90 degree. Decreasing 20% of the power does not have any significant effect on Max. of the residual stresses and it changes between 2% to 6%.

3.3 Effects of Heat Treatment

Comparison of Fig. 5.a and 5.b shows effects of heat treatment on residual stresses of different conditions. Also, comparison of Fig. 5.c and 5.d shows the effects of heat treatment on distortion of the process. By considering results, it shows that heat treatment is mostly help the process for reducing distortion in most of the conditions approximately.

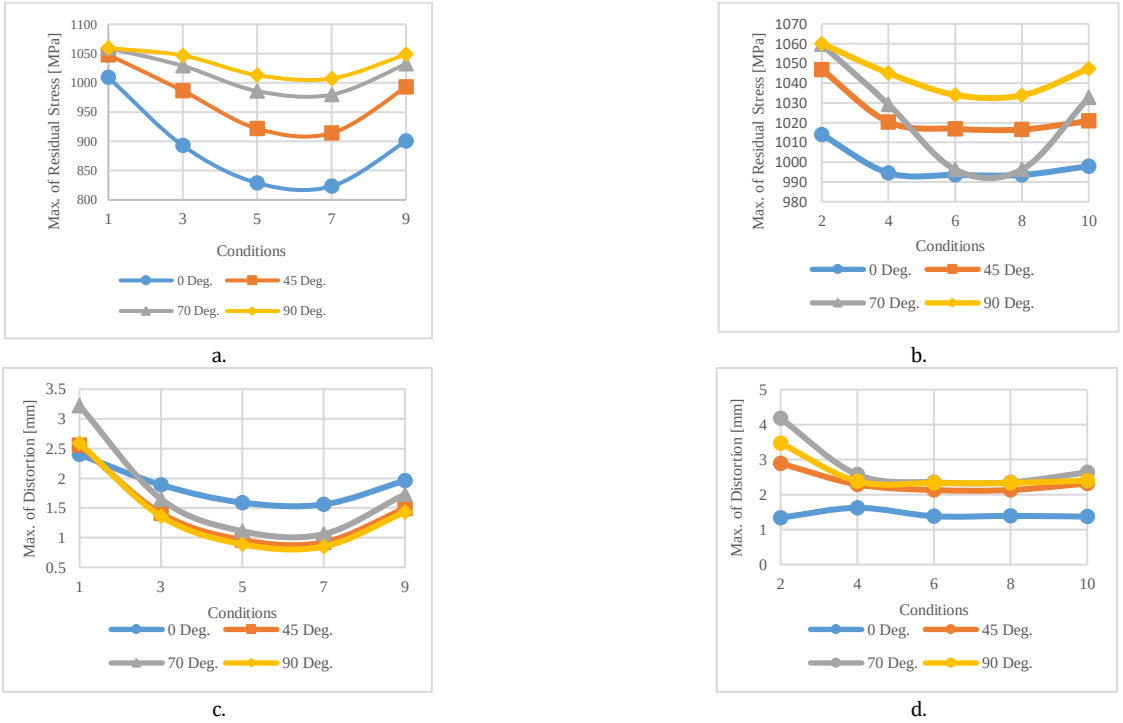

Figure 5: a. Max. of residual Stress without heat treatment, b. Max. of residual Stress with heat treatment, c. Max. of distortion without heat treatment, d. Max. of distortion with heat treatment

4. Conclusions

SLM manufacturing of IN718 pump impeller in 0 degree has the least residual stress, distortion and layers displacement, and 90 degree has the most residual stress between considered situations. Increasing the speed for about 20% decline residual stress and distortion for about 34% from the initial condition and it reaches up to 65% in 90 degree. Decreasing 20% of the speed and increasing 20% to the power have almost same results and caused reduction of the residual stress for about 11% in 0 degree, but this effect become faded continuously by increasing the main part orientation to 90 degree. By reducing 20% of the power, there is not any significant reduction in Max. residual stresses and distortion of the process. Heat treatment shows positive effects on reduction of distortion of the manufactured part but the effects on residual stresses are not significant.

References

A Aminifar, A M. Haghighi, 2020. Effects Of Welding Current And Speed On Residual Stress And Distortion Of Joining St52 Rolled Plate In Different Welding Sequences. Acta Mechanica Malaysia, 3(2): 43-48.

A. Wu, D. Brown, M. Kumar, G. Gallegos and W. King, 2014, An Experimental Investigation into Additive Manufacturing-Induced Residual Stresses in 316L Stainless Steel, Metallurgical and Materials Transactions A, vol. 45, no. 13, pp. 6260-6270. Available: 10.1007/s11661-014-2549-x.

B, Ahmed, van der Veen, S, Fitzpatrick, M & Guo, H, 2018, Residual Stress Evaluation in Selective-Laser-Melting Additively Manufactured Titanium (Ti-6Al-4V) and Inconel 718 using the Contour Method and Numerical Simulation. Additive Manufacturing, vol 22, pp. 571-582.

F. Hajializadeh and A. Ince, 2019, Finite element–based numerical modeling framework for additive manufacturing process, Material Design & Processing Communications, vol. 1, no. 1, p. e28. Available: 10.1002/mdp2.28.

H, Liu, T, Sparks, F, Liou, 2015. Residual Stress and Deformation Modelling for Metal Additive Manufacturing Processes. Proceedings of the World Congress on Mechanical, Chemical, and Material Engineering (MCM 2015), 245.

H. Attia, S. Tavakoli, R. Vargas and V. Thomson, 2010, Laser-assisted high-speed finish turning of superalloy Inconel 718 under dry conditions, CIRP Annals, vol. 59, no. 1, pp. 83-88. Available: 10.1016/j.cirp.2010.03.093.

H. Zhang, S. Zhang, M. Cheng and Z. Li, 2010, Deformation characteristics of δ phase in the delta-processed Inconel 718 alloy, Materials Characterization, vol. 61, no. 1, pp. 49-53. Available: 10.1016/j.matchar.2009.10.003.

J. Cao, M. Gharghouri and P. Nash, 2016. Finite-element analysis and experimental validation of thermal residual stress and distortion in electron beam additive manufactured Ti-6Al-4V build plates, Journal of Materials Processing Technology, vol. 237, pp. 409-419, Available: 10.1016/j.jmatprotec.2016.06.032. Available: 10.1016/j.ijmecsci.2017.12.001.

J. Costes, Y. Guillet, G. Poulachon and M. Dessoly, 2007, Tool-life and wear mechanisms of CBN tools in machining of Inconel 718, International Journal of Machine Tools and Manufacture, vol. 47, no. 7-8, pp. 1081-1087. Available: 10.1016/j.ijmachtools.2006.09.031.

M. Anderson, R. Patwa and Y. Shin, 2006, Laser-assisted machining of Inconel 718 with an economic analysis, International Journal of Machine Tools and Manufacture, vol. 46, no. 14, pp. 1879-1891. Available: 10.1016/j.ijmachtools.2005.11.005.

Mercelis and J. Kruth, 2006, Residual stresses in selective laser sintering and selective laser melting, Rapid Prototyping Journal, vol. 12, no. 5, pp. 254-265. Available: 10.1108/13552540610707013.

NC Levkulich, Semiatin SL, Gockel JE, Middendorf JR, DeWald AT, Klingbeil NW, 2019, The Effect of Process Parameters on Residual Stress Evolution and Distortion in the Laser Powder Bed Fusion of Ti-6Al-4V, Additive Manufacturing. https://doi.org/10.1016/j.addma.2019.05.015

O. Fergani, F. Berto, T. Welo and S. Liang, 2016, Analytical modelling of residual stress in additive manufacturing, Fatigue & Fracture of Engineering Materials & Structures, vol. 40, no. 6, pp. 971-978. Available: 10.1111/ffe.12560.

P. Bian, J. Shi, Y. Liu and Y. Xie, 2020, Influence of laser power and scanning strategy on residual stress distribution in additively manufactured 316L steel, Optics & Laser Technology, vol. 132, p. 106477. Available: 10.1016/j.optlastec.2020.106477.

R. Rashid et al., 2018, Effect of energy per layer on the anisotropy of selective laser melted AlSi12 aluminium alloy, Additive Manufacturing, vol. 22, pp. 426-439. Available: 10.1016/j.addma.2018.05.040.

T. Mukherjee, W. Zhang and T. DebRoy, 2017, An improved prediction of residual stresses and distortion in additive manufacturing", Computational Materials Science, vol. 126, pp. 360-372. Available: 10.1016/j.commatsci.2016.10.003.

X., Zhao, A., Iyer, P., Promoppatum, & S. C, Yao, 2017. Numerical modeling of the thermal behavior and residual stress in the direct metal laser sintering process of titanium alloy products. Additive Manufacturing, 14, 126-136.

Y. Li, K. Zhou, P. Tan, S. Tor, C. Chua and K. Leong, 2018, Modeling temperature and residual stress fields in selective laser melting, International Journal of Mechanical Sciences, vol. 136, pp. 24-35.

Z. Wang, K. Guan, M. Gao, X. Li, X. Chen and X. Zeng, 2012, The microstructure and mechanical properties of deposited-IN718 by selective laser melting. Journal of Alloys and Compounds, vol. 513, pp. 518-523. Available: 10.1016/j.jallcom.2011.10.107.